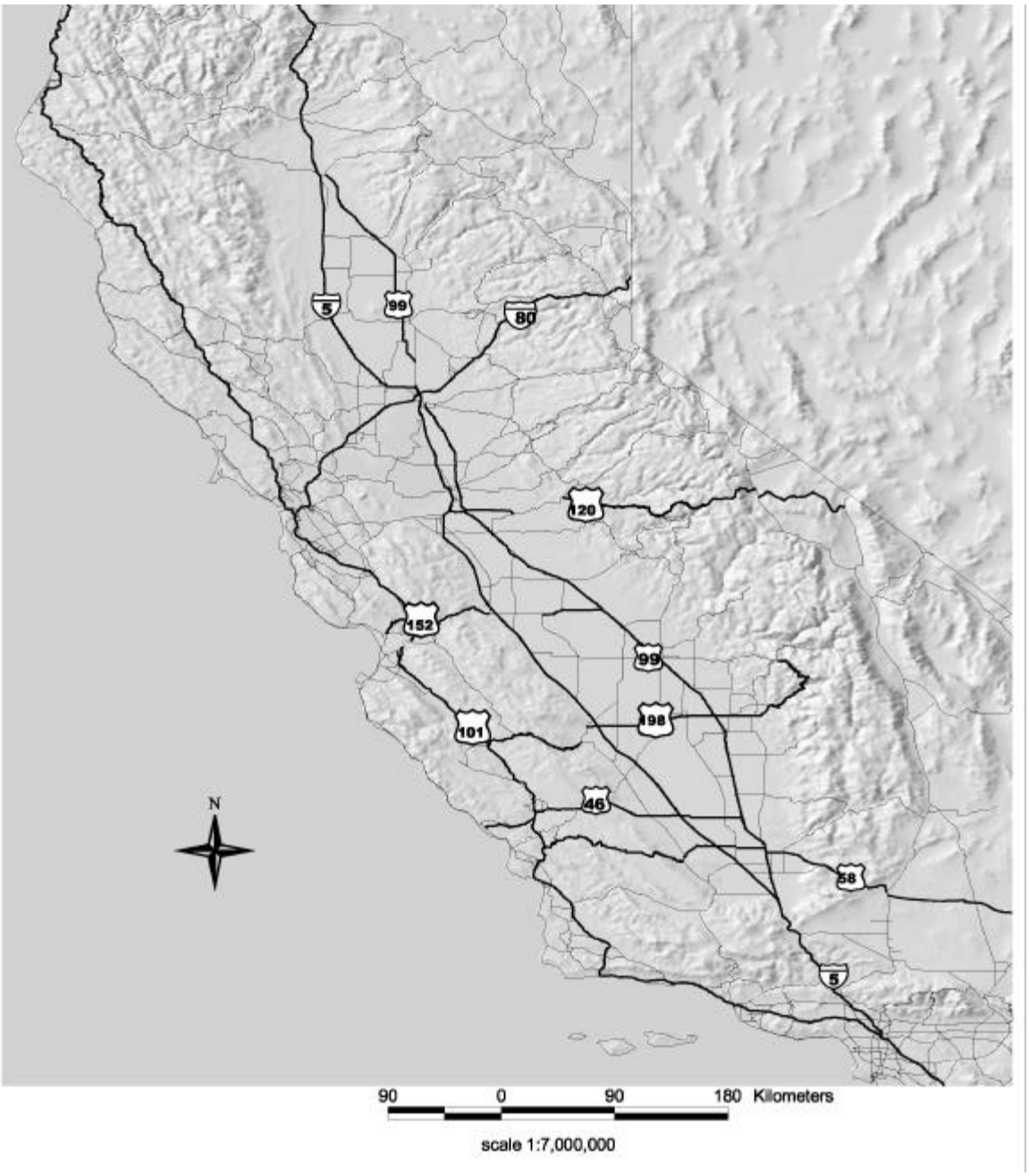

Figure 2.1-5. Major highway routes in central California.

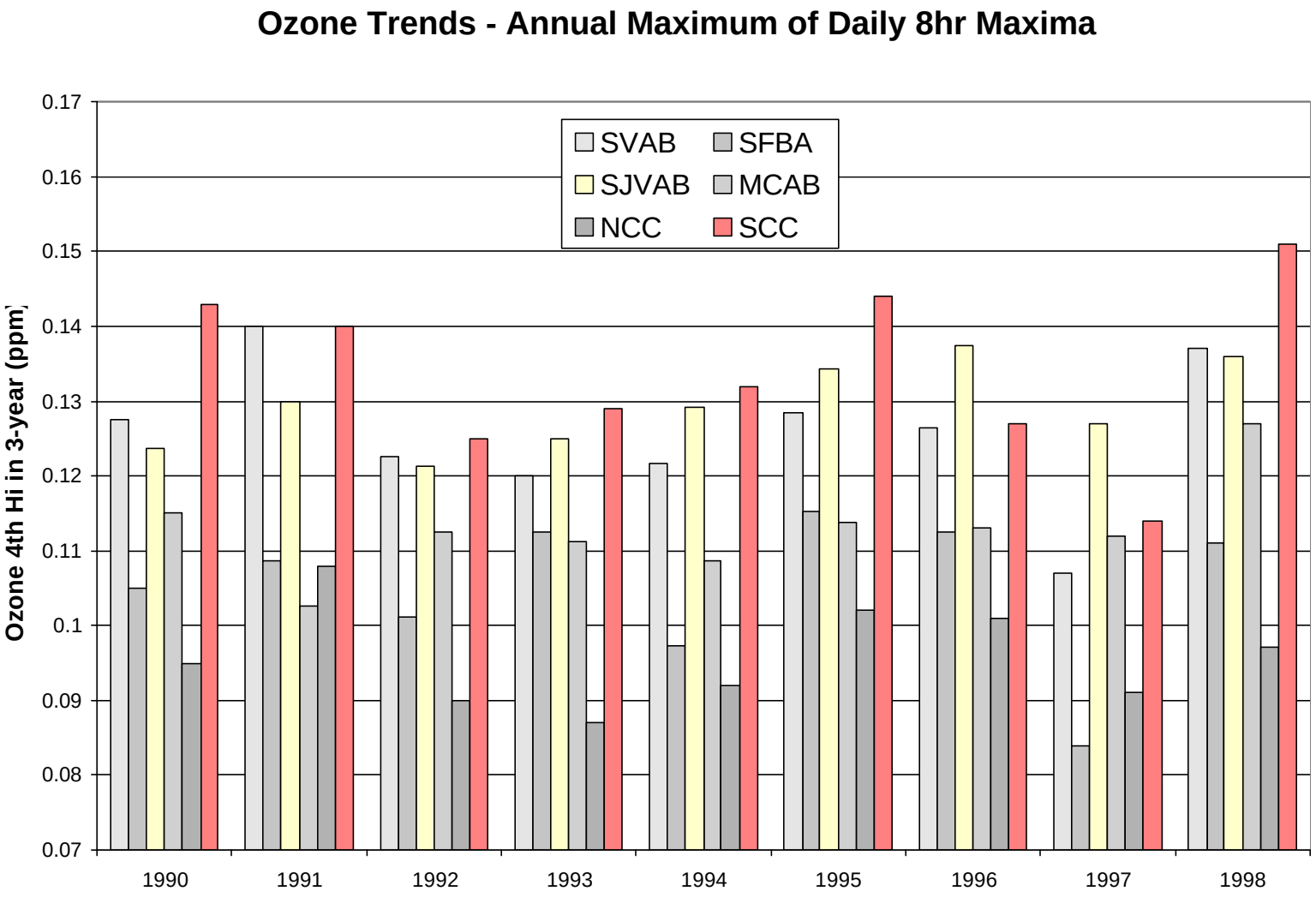

Figure 2.3-1. Annual basin maximum of 8-hour daily maximum ozone trends by location type.

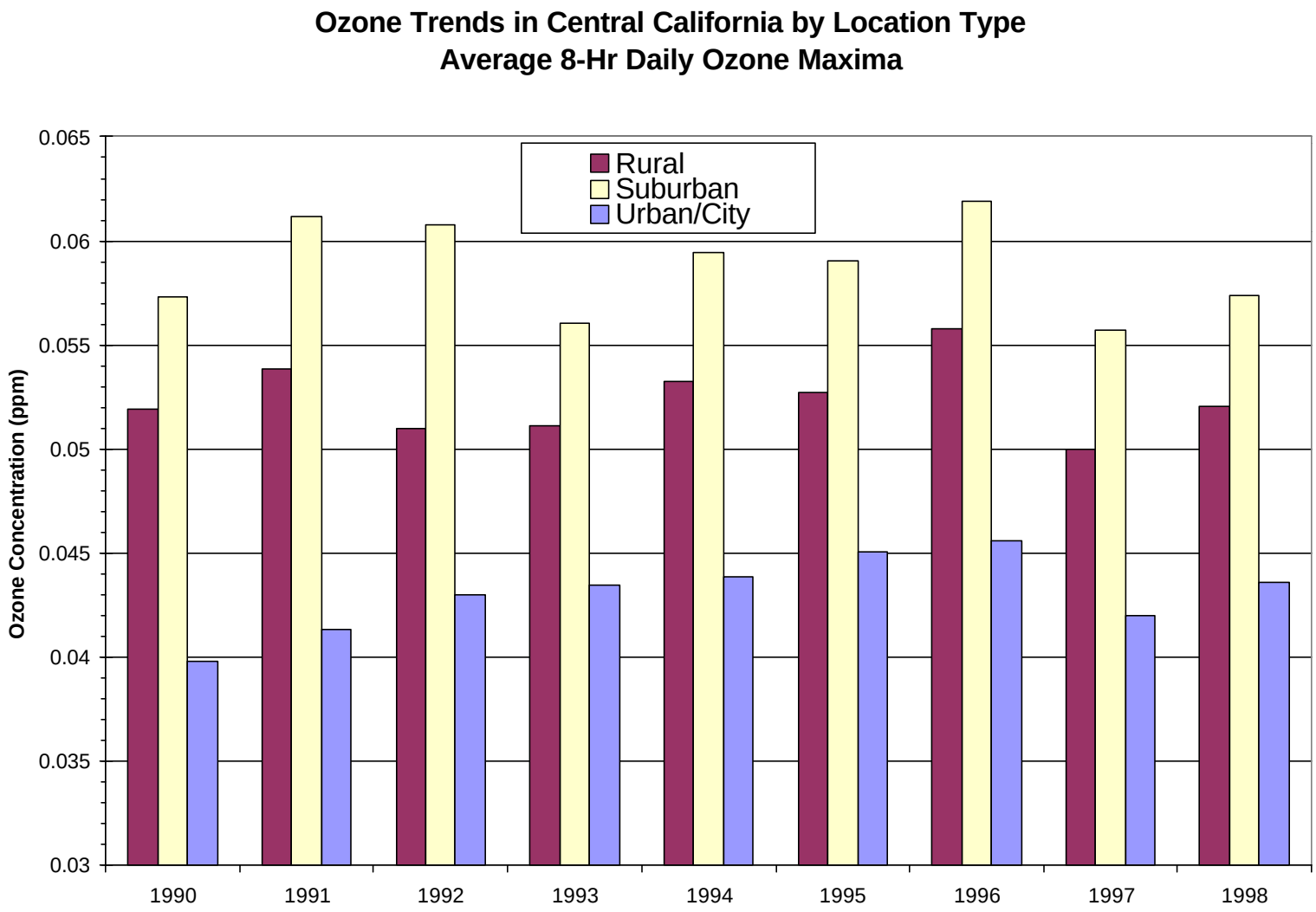

Figure 2.3-2. Average 8-hour daily maximum ozone trends in central California by location type.

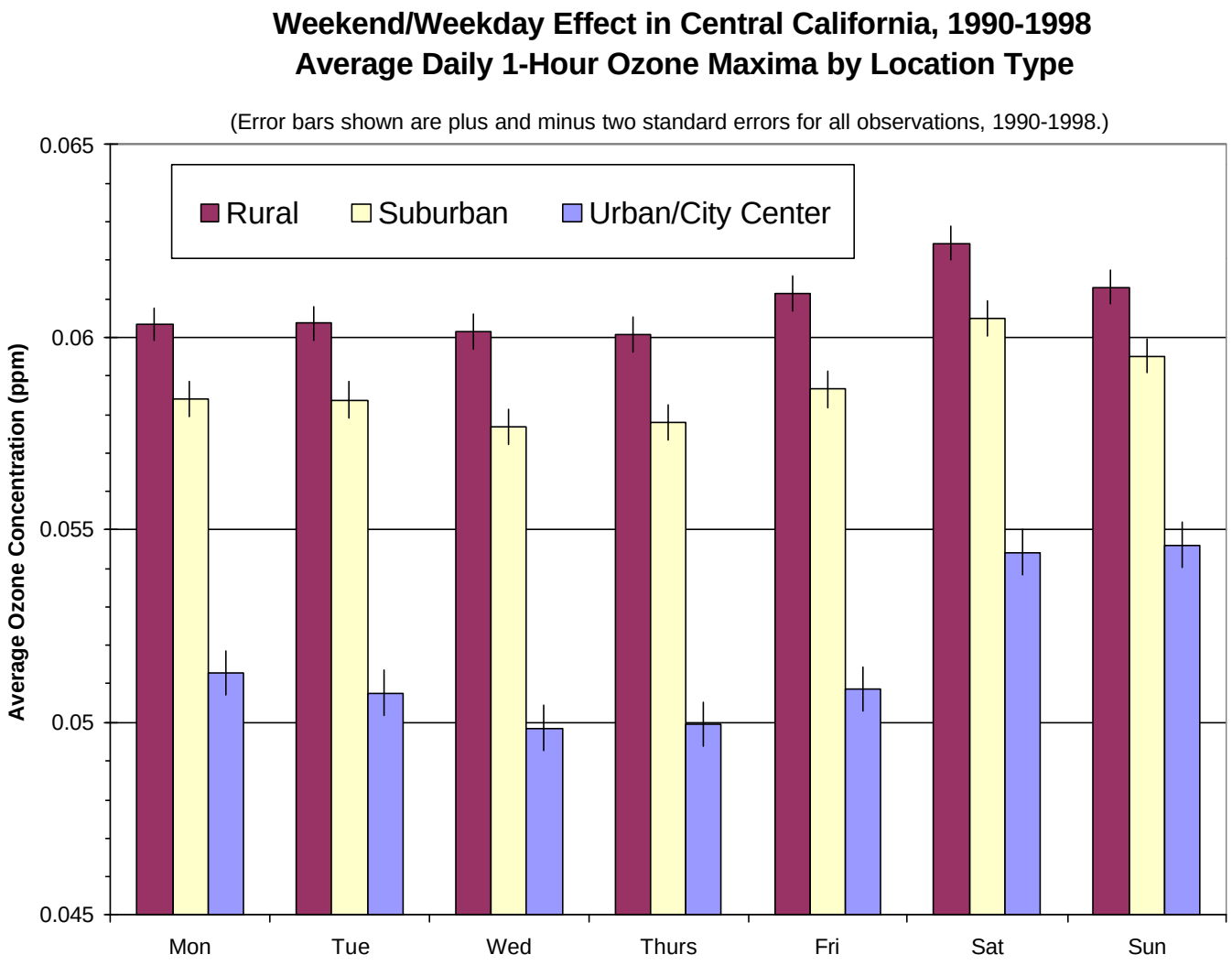

Figure 2.3-3. Weekend/weekday effect on average 1-hour daily maximum ozone in central California by location type.

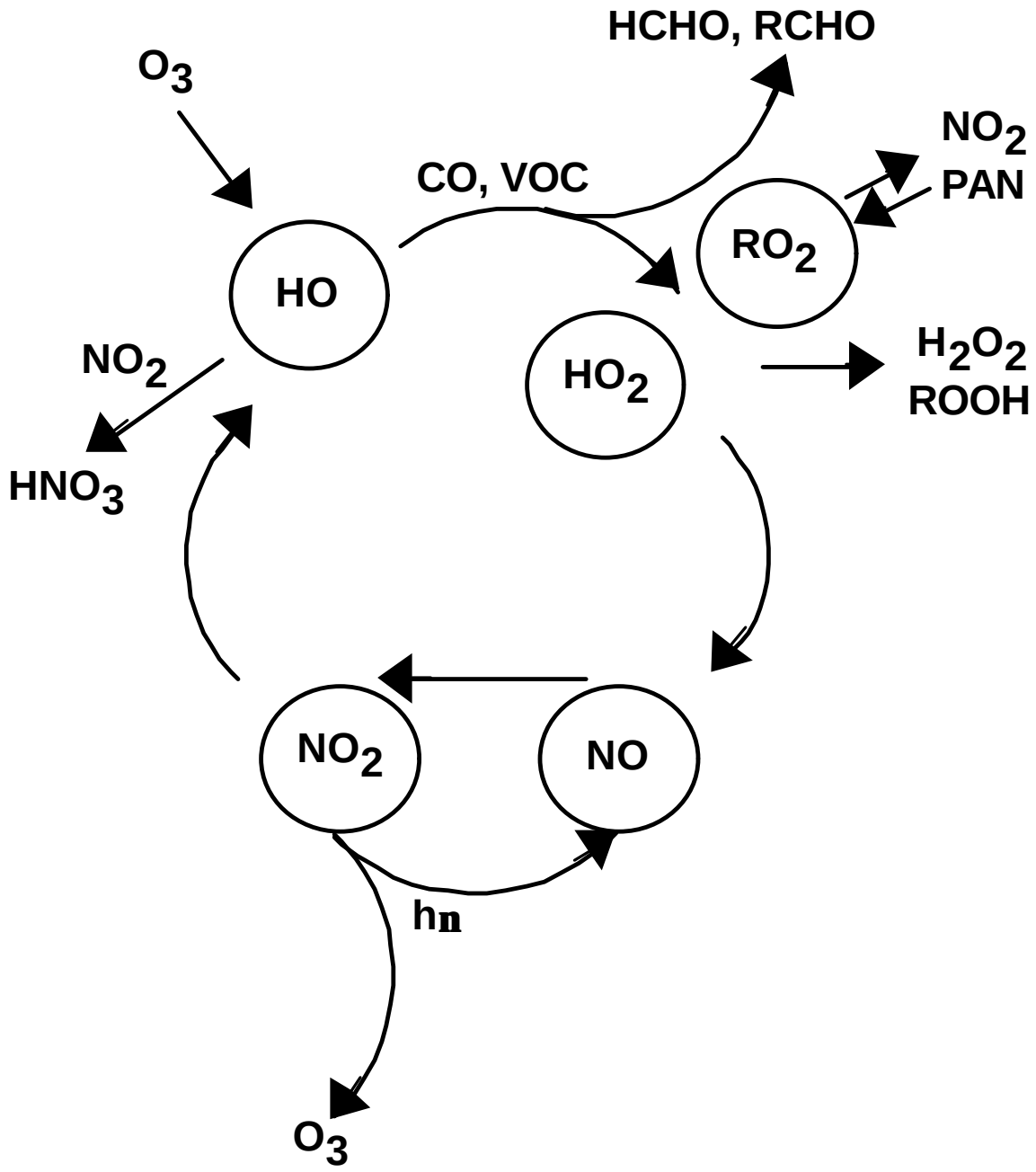

Figure 2.6-1. Overview of ozone production in the troposphere.

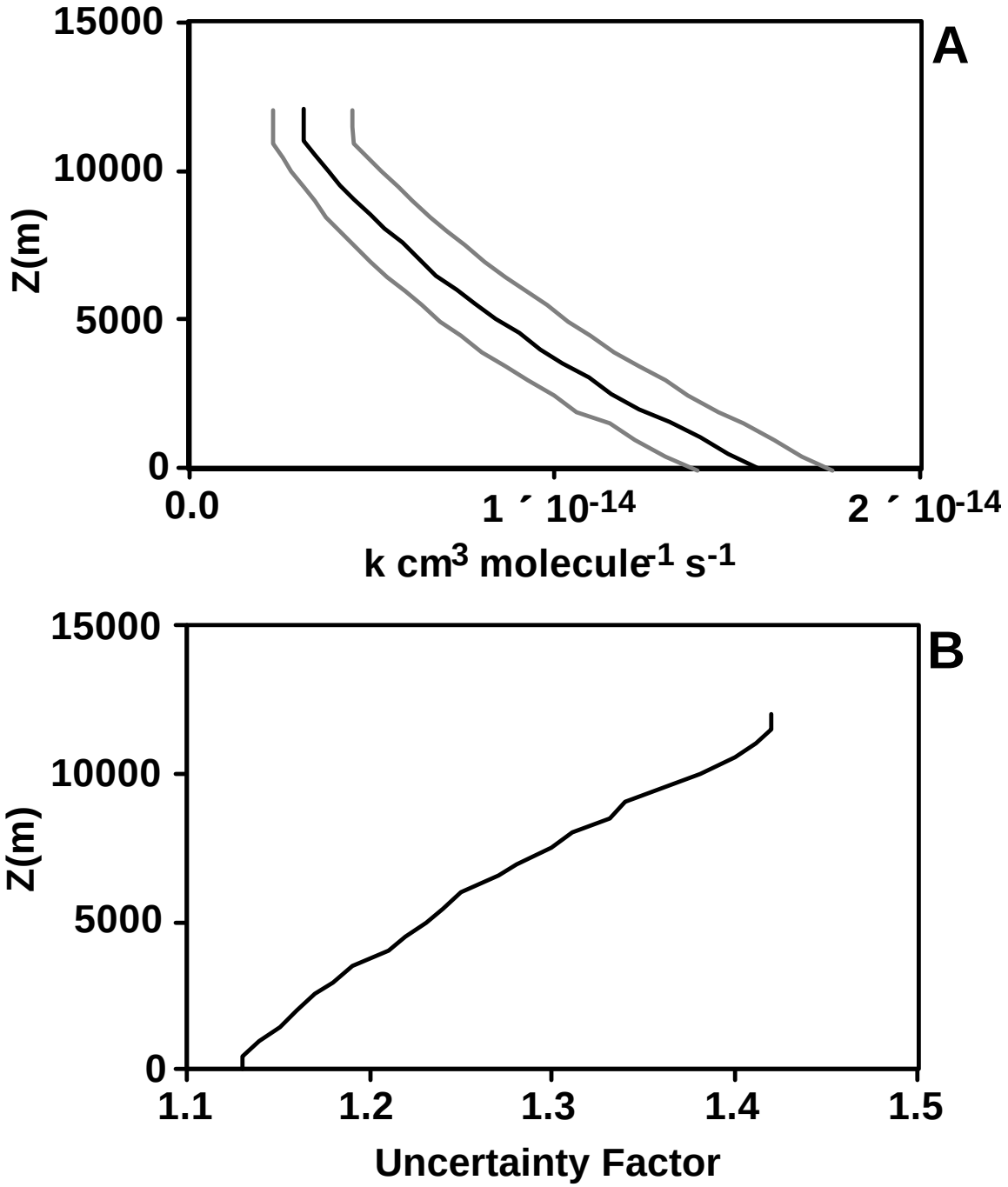

Figure 2.6-2. (A) Rate constant for the O_3 + NO reaction with upper and lower bounds. (B) The uncertainty factor, f(T). Data are from DeMore et al. (1997).

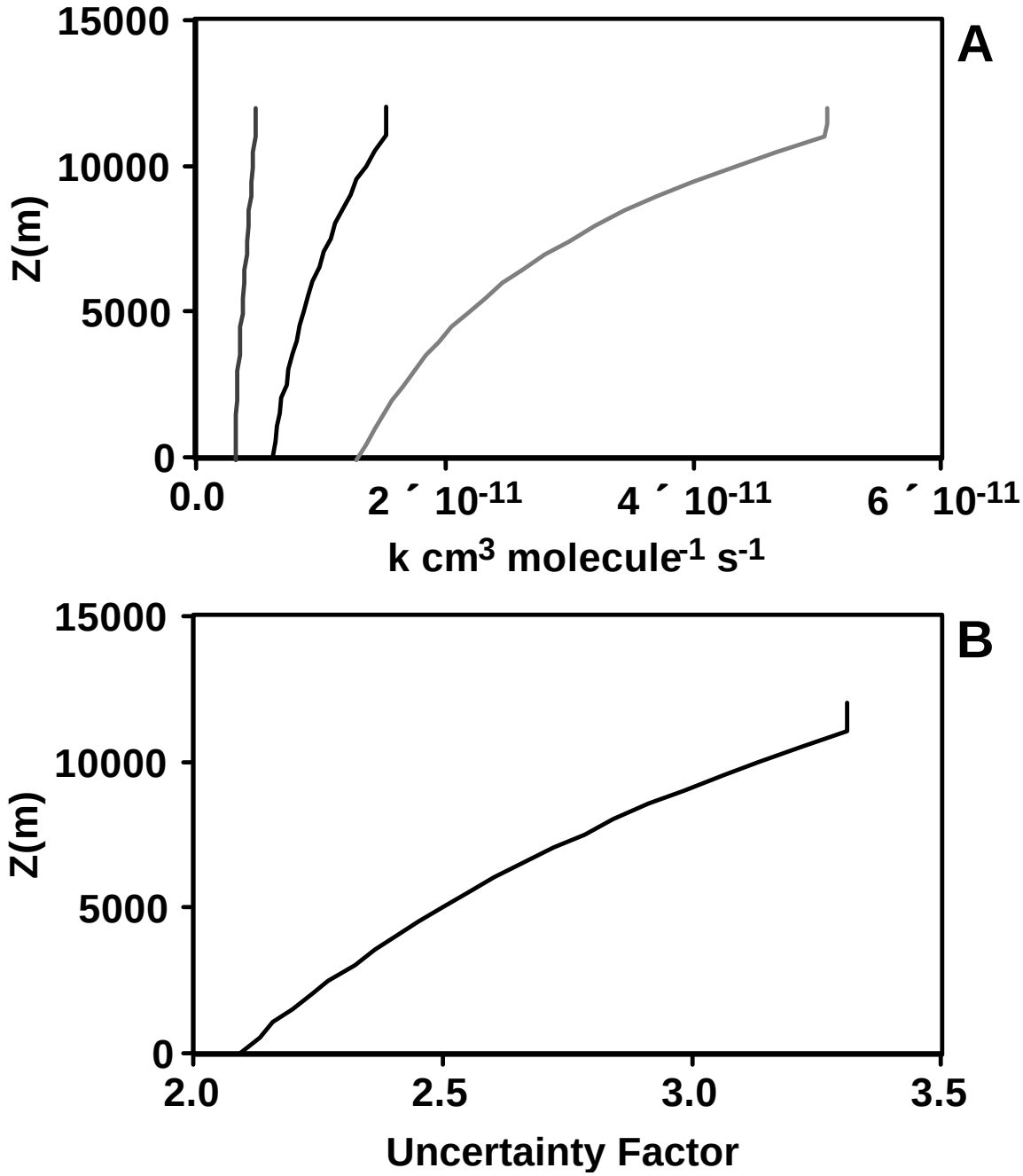

Figure 2.6-3. (A) Rate constant for the CH_3O_2 + HO_2 reaction with upper and lower bounds. (B) The uncertainty factor, f(T). Data from DeMore et al. (1997).

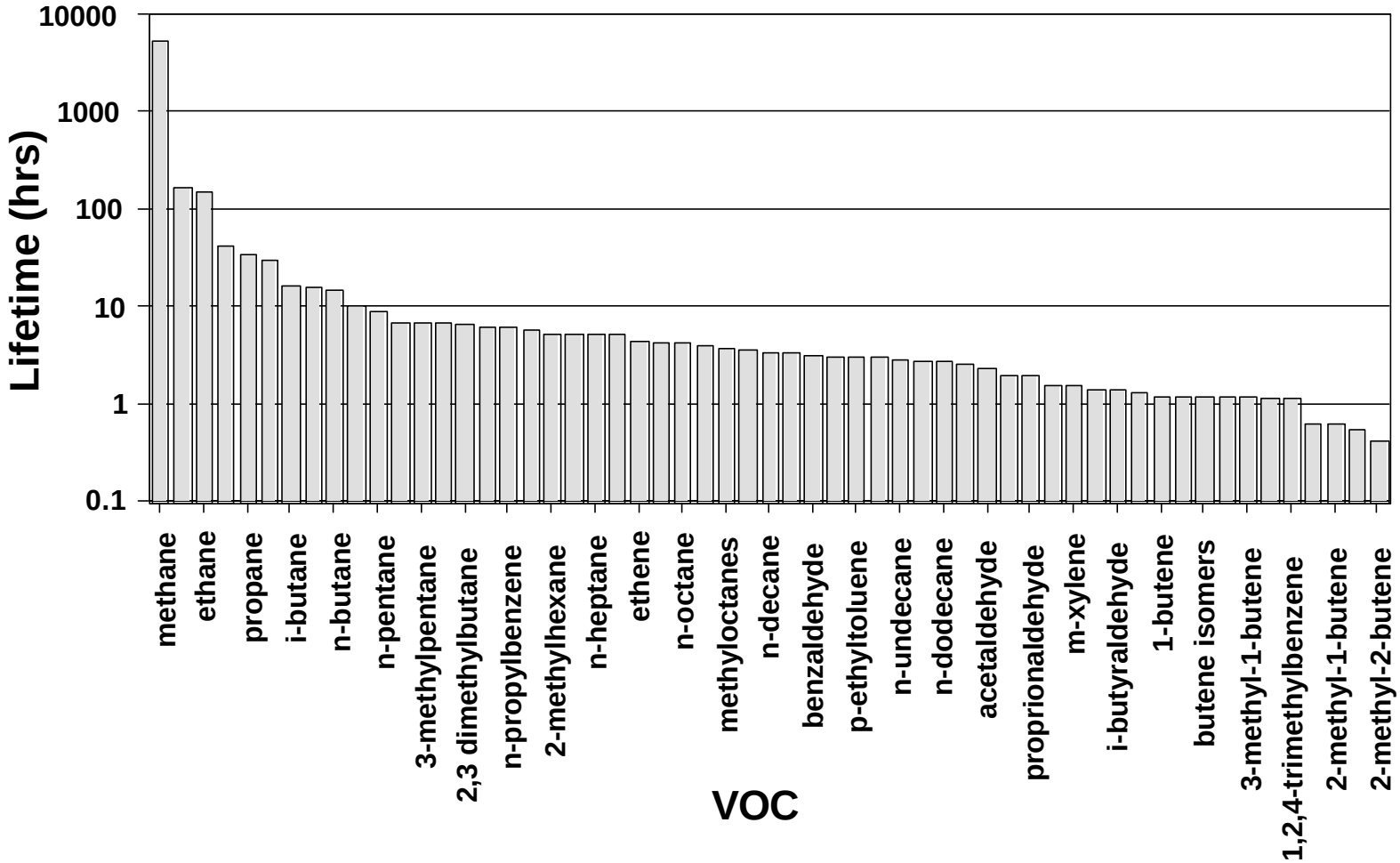

Figure 2.6-4. Atmospheric lifetimes of selected organic compounds with respect to a hydroxyl radical concentration of 7.5×10^6 molecules cm^{-3}.

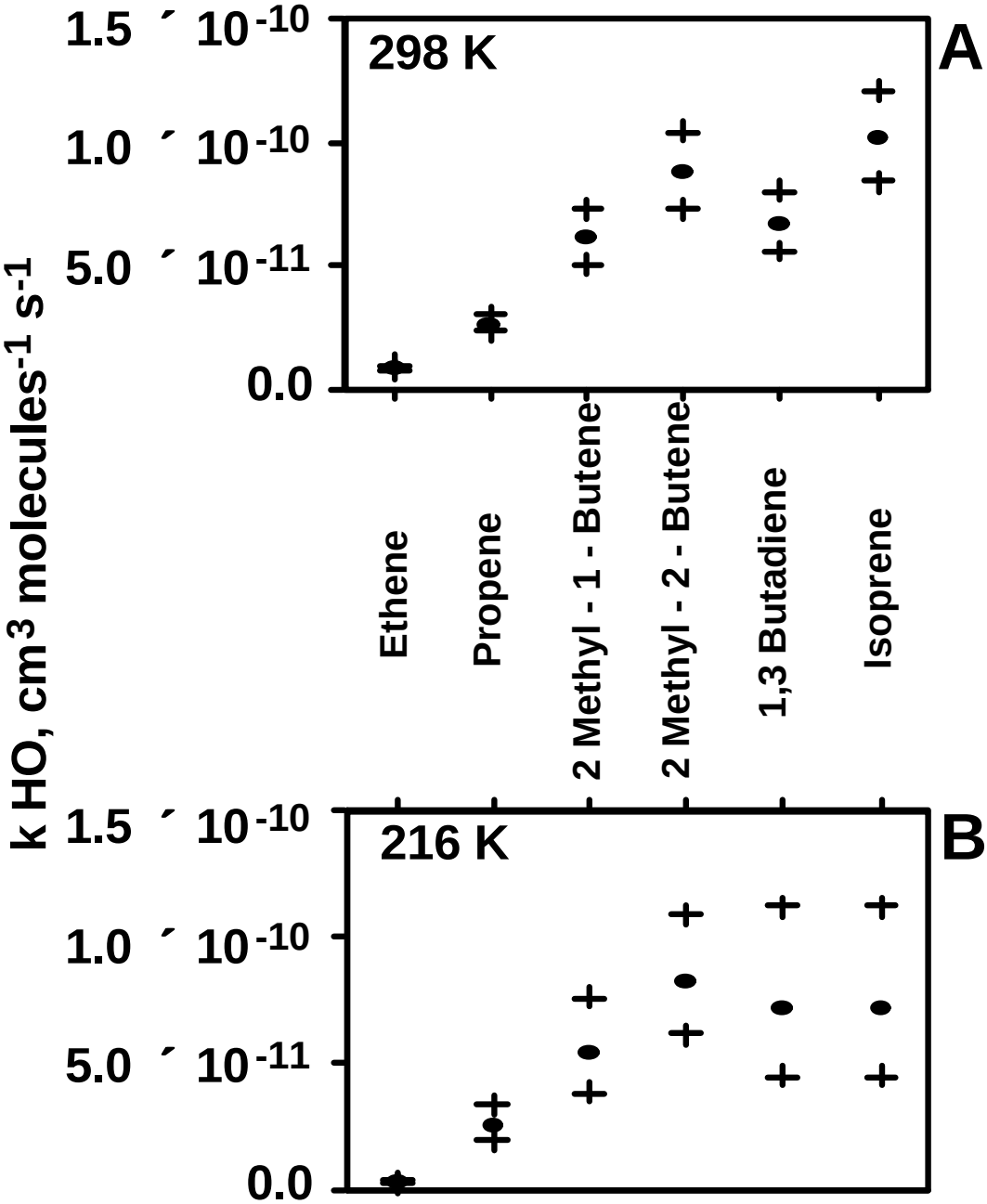

Figure 2.6-5. Uncertainties in rate parameters for HO radical reactions with alkenes. The closed circles represent the nominal value while the crosses represent the approximate 1σ; (A) 298 K; (B) 216 K.

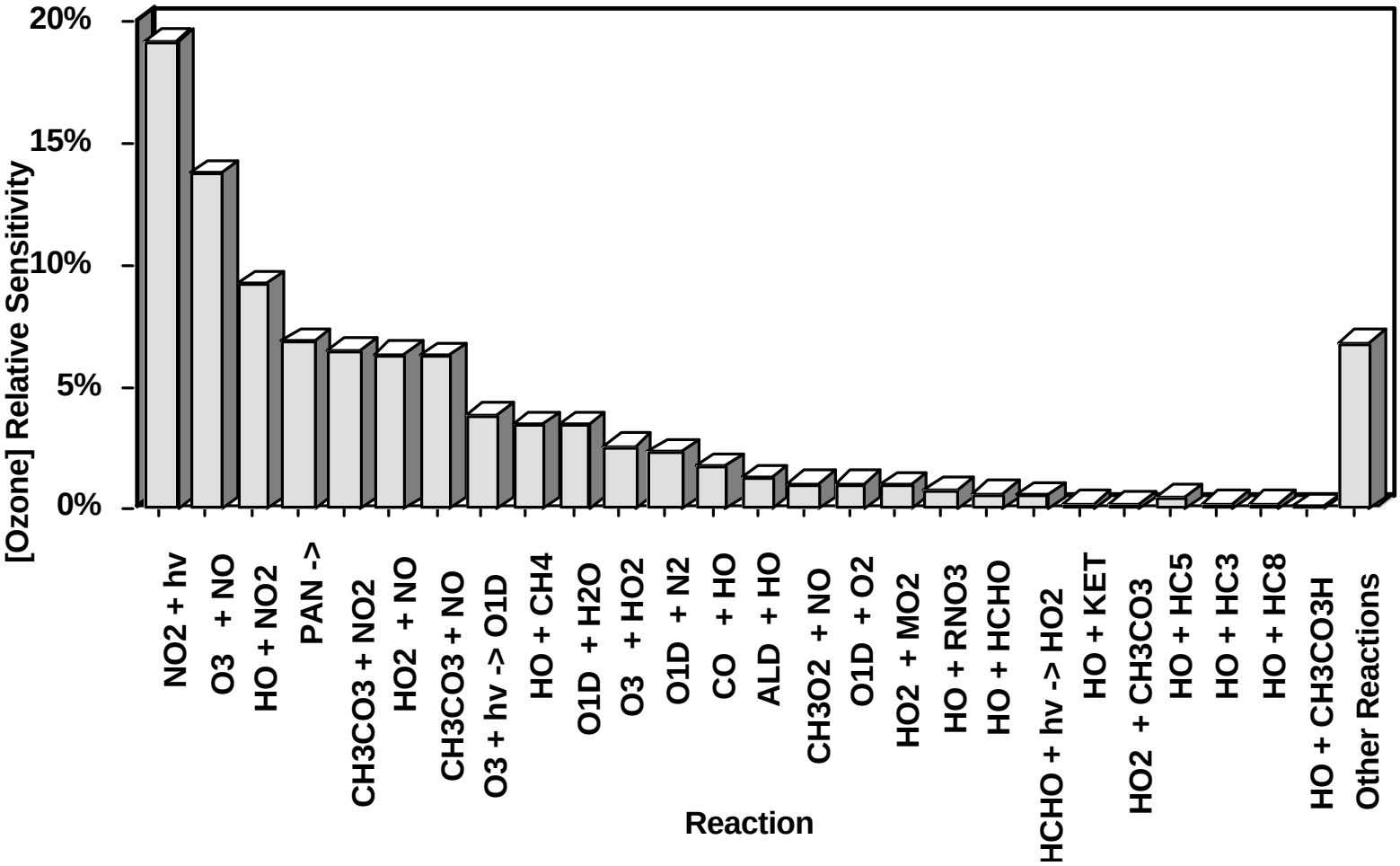

Figure 2.6-6. Relative sensitivity of ozone to reaction rate constants. Initial total reactive nitrogen concentration is 2 ppb and total initial organic compound concentration is 50 ppbC (Stockwell et al. 1995).

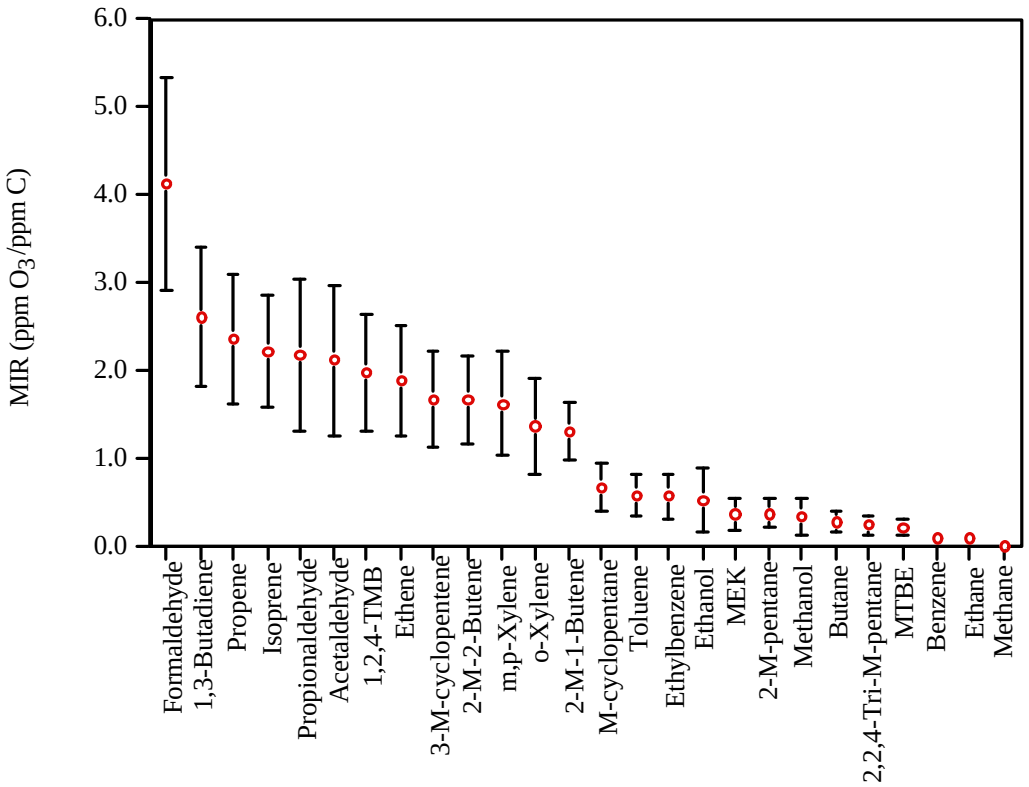

Figure 2.6-7. Mean values and 1σ uncertainties of maximum incremental reactivity values for selected hydrocarbons determined from Monte Carlo simulations (Yang et al., 1995).

Figure 2.8-1. Plot of 1-hr ozone concentrations over central California at noon on the second simulated day. The area directly west of the San Francisco Bay Area has ozone concentrations near 120 ppb while high ozone concentrations are found along and directly west of the San Joaquin valley.

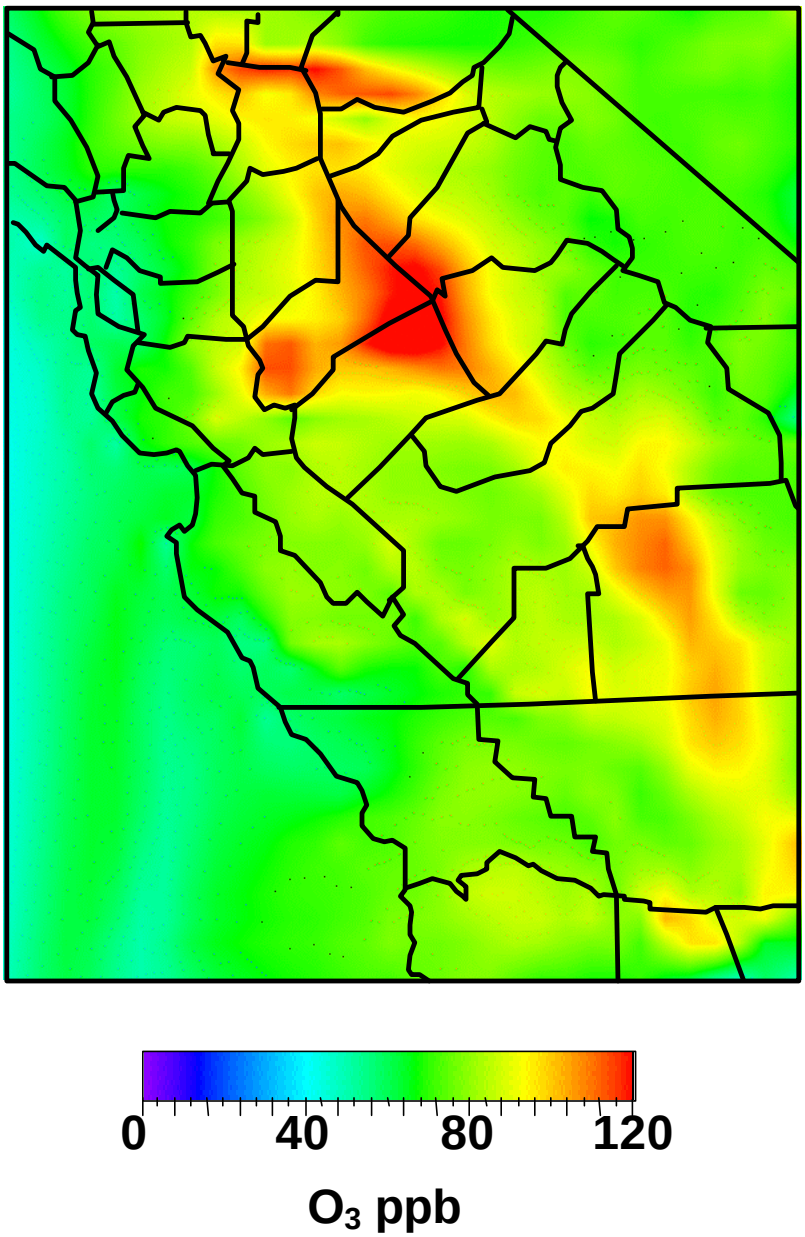

Figure 2.8-2. Plot of 1-hr ozone concentrations in central California at midnight after two simulated days. Note that the western boundary and the San Joaquin Valley have ozone concentrations near 40 ppb or less.

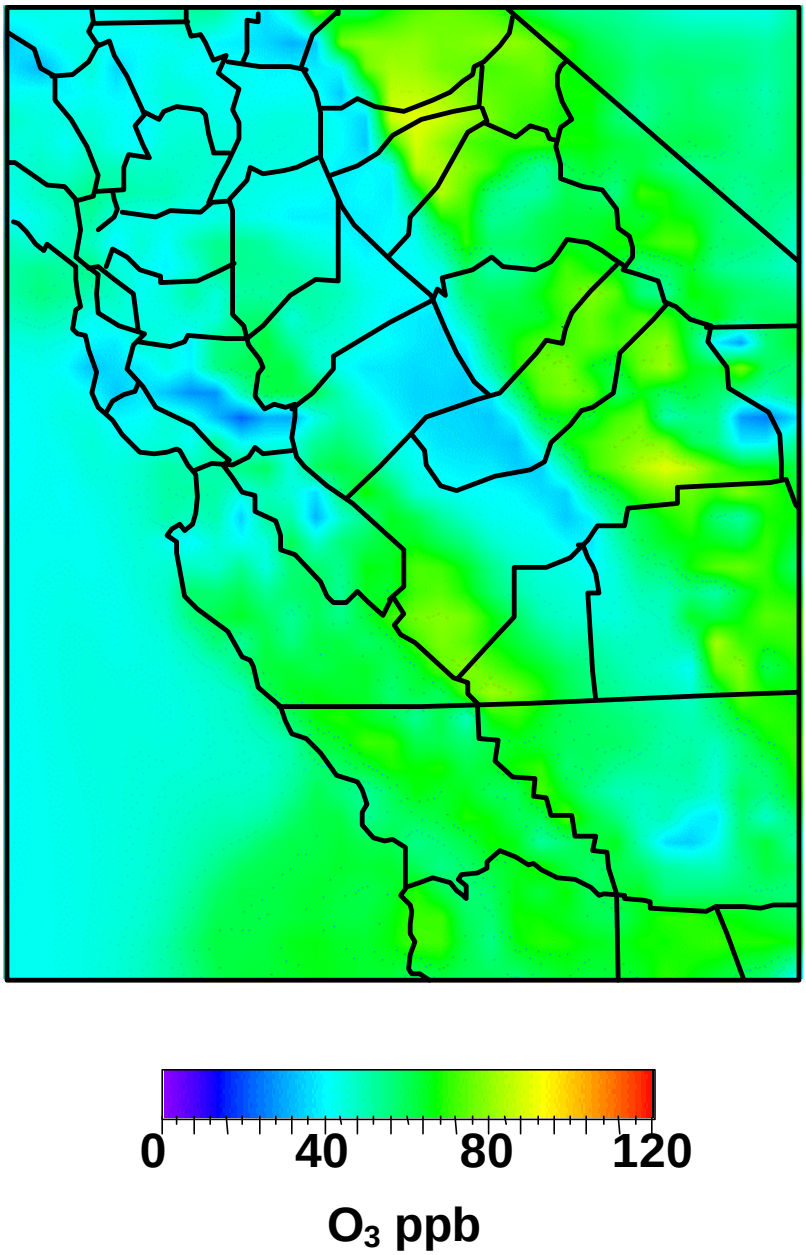

Figure 2.8-3. Plot of 1-hr ozone concentrations in central California at noon on the third simulated day. The high ozone pattern is more complicated with several ozone hot spots one directly west of the San Francisco Bay Area with two more directly to the north and south. High ozone concentrations are found also along and directly west and south of the San Joaquin valley.

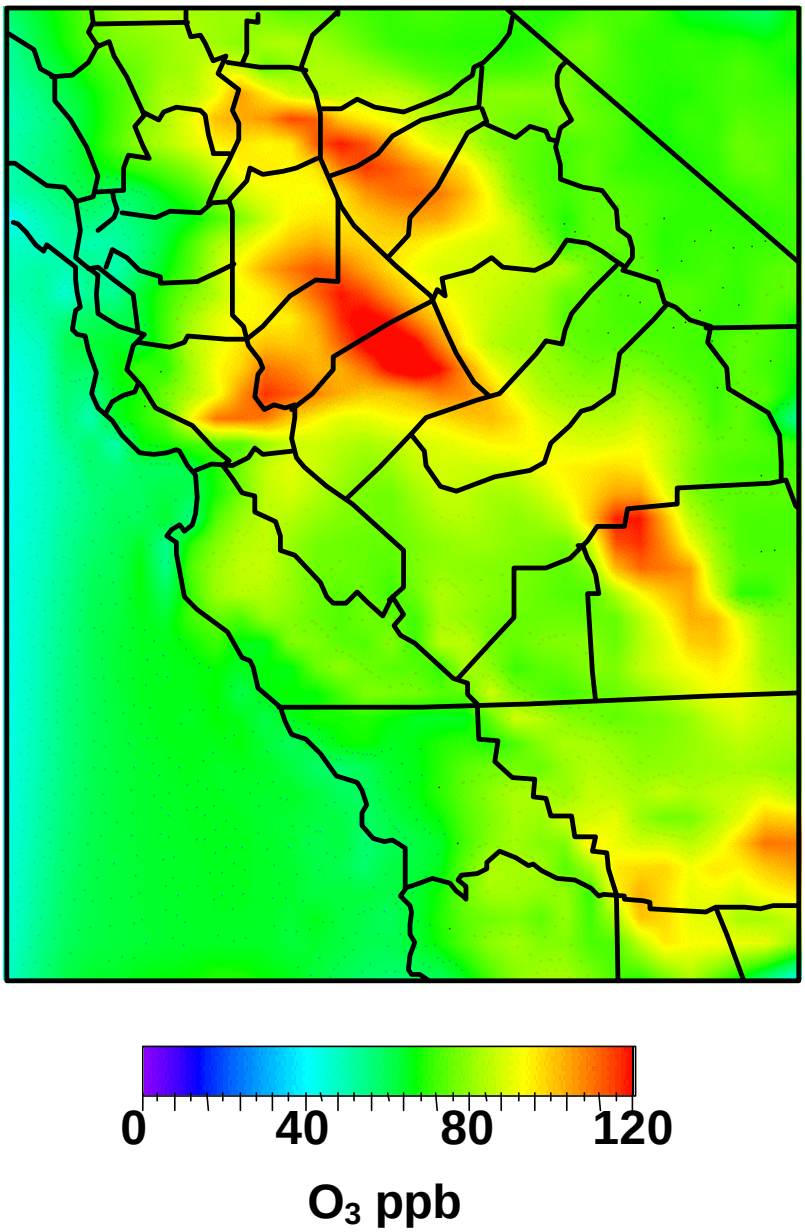

Figure 2.8-4. Plot of 1-hr ozone concentrations in the vertical along a north – south cross section through the center of central California. The vertical coordinate is linear in pressure following coordinates which exaggerates the apparent height. Plot A shows the ozone concentrations at noon on the second day and Plot B shows the ozone concentrations at midnight after two simulated days. The high ozone concentrations at noon, Plot A, and the low ozone concentrations at midnight, Plot B, are found over the Sacramento area.

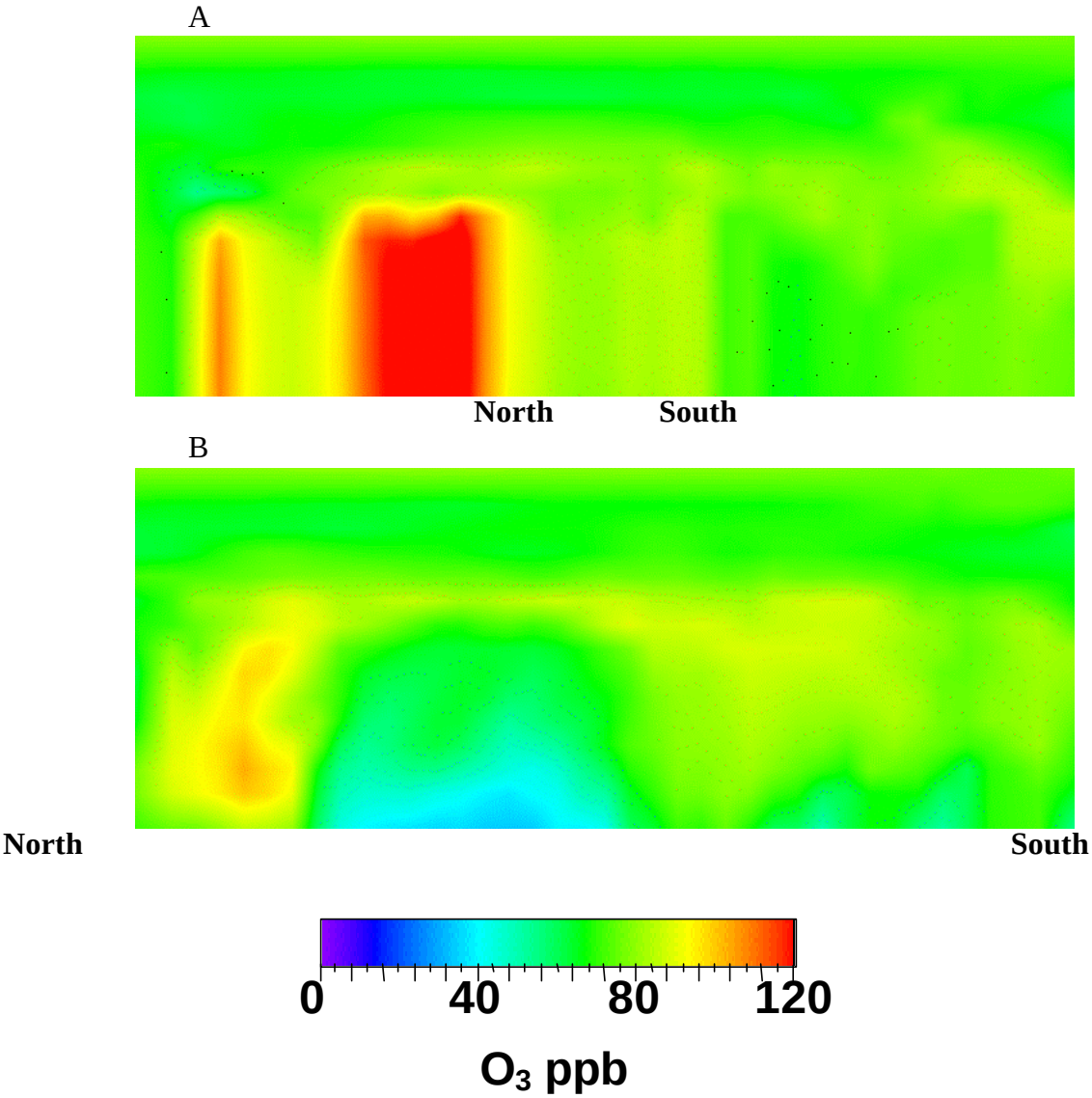

Figure 2.8-5. Plot of 1-hr ozone concentrations in the vertical along a west – east cross section through central California along a line running from the San Francisco Bay Area through Sacramento to the front range. The vertical coordinate is linear in pressure following coordinates which exaggerates the apparent height. Plot A shows the ozone concentrations at noon on the second day, Plot B shows them at 6:00 PM on the second day and Plot C shows them at midnight after two simulated days. The plots show evidence of transport of ozone and NO_x from the west to the east.

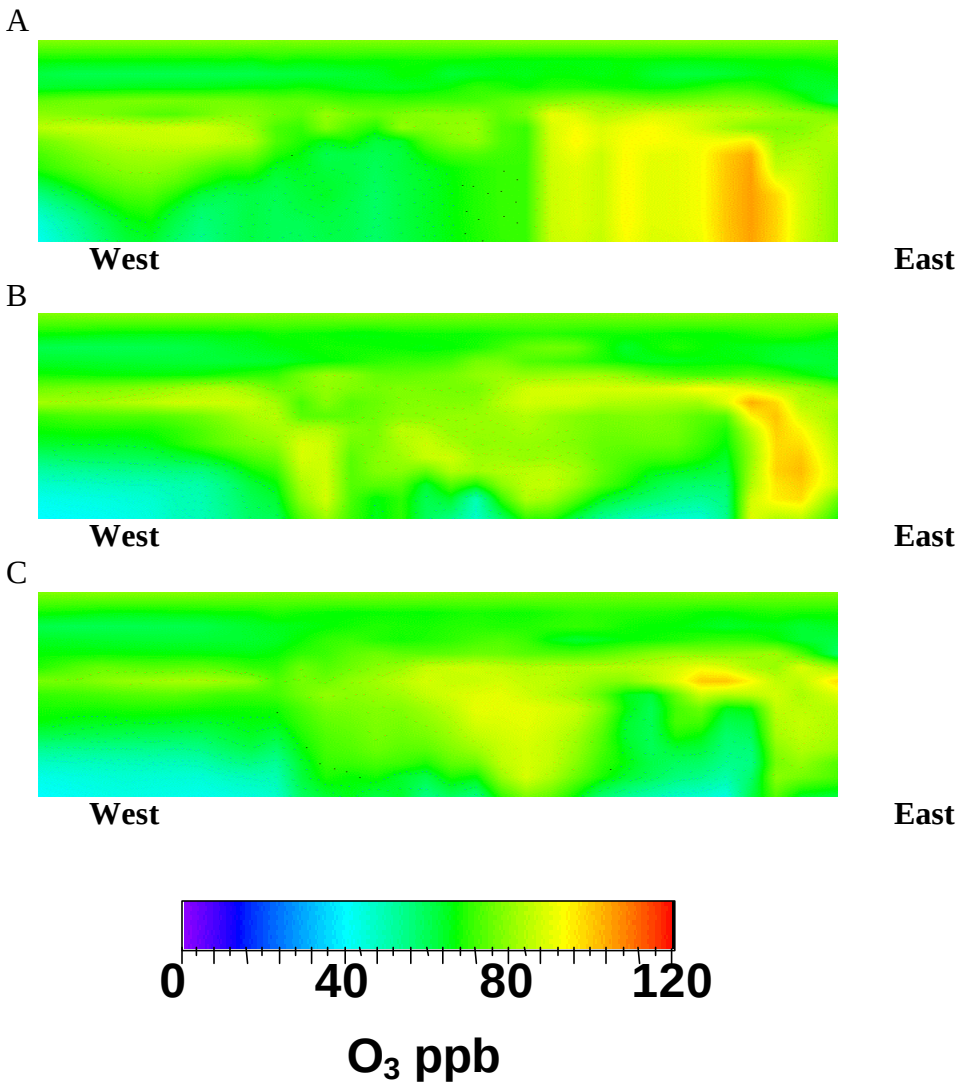

Figure 2.8-6. Plot of formaldehyde concentrations at midnight after two simulated days. Note that the western boundary has around 5 ppb of HCHO. These high HCHO concentrations appear to be due to transport from the model's boundary.

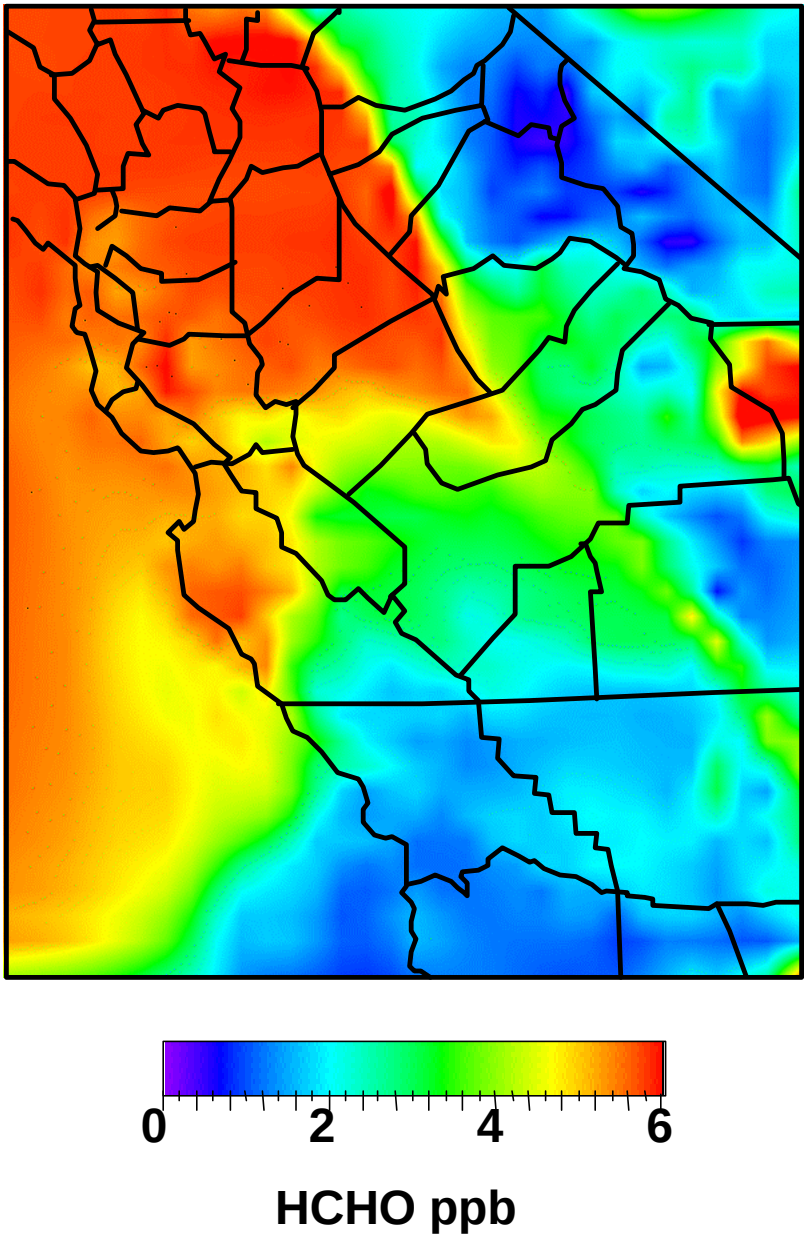

Figure 2.8-7. Plot of NO concentrations at 1:00 PM on the second simulated day. Note that the western boundary has over 0.5 ppb of NO. These moderate NO concentrations for over the ocean appear to be due to transport from the model's boundary.

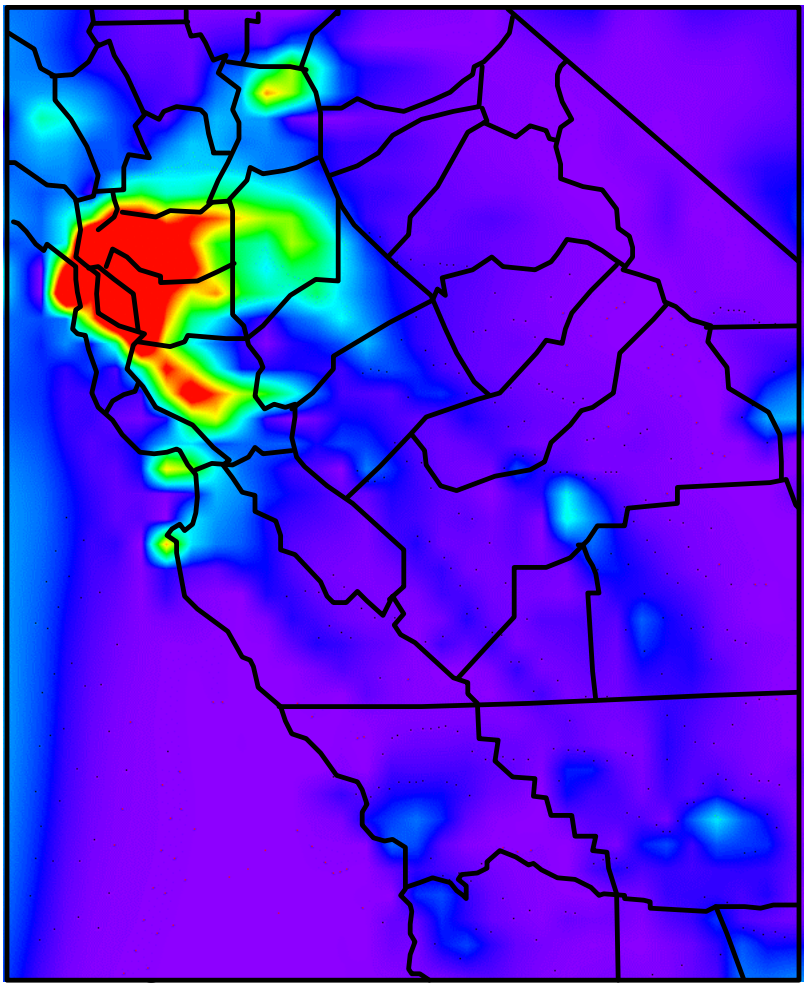

NO ppb